PGC PUBLISHING

Hou Zengqian, Zhong Dalai, Deng Wanming and Khin Zaw, 2005 - A Tectonic Model for Porphyry Copper-Molybdenum-Gold Deposits in the Eastern Indo-Asian Collision Zone; *in Porter, T.M. (Ed.), Super Porphyry Copper & Gold Deposits: A Global Perspective*; PGC Publishing, Adelaide, v. 2, pp 423-440.

A TECTONIC MODEL FOR PORPHYRY COPPER-MOLYBDENUM-GOLD DEPOSITS IN THE EASTERN INDO-ASIAN COLLISION ZONE

[1]Hou Zengqian, [2]Zhong Dalai, [2]Deng Wanming and [3]Khin Zaw

[1]*Institute of Mineral Resources, Chinese Academy of Geological Sciences, Beijing, P.R. China*
[2]*Institute of Geology and Geophysics, Chinese Academy of Sciences, Beijing, P.R. China*
[3]*Centre for Ore Deposit Research, University of Tasmania, Private Bag 79, Hobart,, Australia 7001*

Abstract: Two Himalayan porphyry copper-molybdenum-gold belts have been developed in the eastern part of the Himalayan-Tibet orogenic zone related to the collision between the Indian and Asian Plates. Both were accompanied by the emplacement of high-level intracontinental, alkali-rich, potassic felsic magmas which produced a huge Cenozoic belt of potassic igneous rock. The emplacement of these magmas was controlled by large-scale strike-slip fault systems, orientated roughly orthogonal to the of the Indo-Asian continental convergence, which adjusted the collisional strain. The Jomda-Markam-Xiangyun copper-molybdenum belt is the western of the two, developed along a narrow zone following the Nanqian thrust, the Jinshajiang fault system, and the Red River shear zone, whereas the eastern, the Zhongdian-Yanyuan-Yao'an porphyry copper-gold-silver belt, was developed along the western margin of the Yangtze Craton. The ore-bearing porphyries have compositions which include granite, monzogranite, and monzonite, with a small amount of quartz-syenite porphyry. They are distinguished from barren porphyries by their higher SiO_2 (>63 wt %), lower Y (<20 ppm) and their adakitic magma affinity. All alkali-rich porphyries are relatively enriched in large-ion lithophile elements (K, Rb and Ba) and depleted in high-field strength elements (Nb, Ta, Ti and P) with a wide range of Nb/Y ratios. These porphyries also show strong REE fractionation but no obvious negative Eu anomaly, suggesting that possible magma sources underwent metasomatism by fluids derived from an ancient subducted oceanic slab, and the input of small-volumes of melts derived from the asthenosphere. Adakite-like porphyries might originate from the basaltic lower crust, which probably underwent high-pressure (>40 km), low amphibolite-eclogite facies metamorphism during the Indo-Asian continent collision and metasomatism of slab-derived fluids. Amphibolite and garnet- amphibolite xenoliths in alkali-rich porphyries have been interpreted to be samples of such lower-crustal materials. Barren syenite porphyries might have originated from an enriched mantle characterised by the phlogopite peridotite. Trace element and Sr-Nd-Pb isotope systematics of these barren porphyries indicate that their source was subjected to much strong metasomatism by slab-derived fluid and dissemination of the underlying asthenospheric material. Available geophysical data in eastern Tibet suggest that the Yangtze continental slab was subducted westwards since 50 Ma and collided with the subducted Indian continental slab, thus inducing upwelling, thermal erosion and underplating of asthenospheric melts and giving rise to partial melting of the crust-mantle transition zone to produce adakite-like, potassic, felsic magmas. Such magmatic systems are characteristically rich in water and sulphur with high oxygen fugacity (fO_2), which could largely result in the potential for magmatic process to better carry and transport metal and sulphur. The intersection of the large-scale strike-slip faults with basement lineaments controlled the temporal-spatial localisation of porphyry Cu-Mo-Au systems.

Introduction

Sillitoe (1972) and Mitchell (1973) published their pioneering tectonic models for the setting of porphyry copper deposits i.e., porphyry copper deposits occur in island arcs and continental margin arcs along convergent plate boundaries. The model incorporates magma which originated in a mantle wedge, was metasomatised by fluids from the subducted slab and was then subjected to crystallisation differentiation and/or contamination with crustal material in a relatively closed system, resulting in the formation of ore-bearing porphyries and development of a magmatic-hydrothermal Cu system. This model has also been strongly supported by studies of a number of large and super-large porphyry copper-gold deposits discovered in the Circum-Pacific metallogenic belts in the last few decades (Griffiths and Godwin, 1983; Sillitoe and Camus, 1991; Camus and Dilles, 2001). However, porphyry copper deposits not only occur in island and continental margin arcs but also in collisional orogenic belts. Typical examples include the Yulong porphyry copper belt in eastern Tibet (Rui *et al.,* 1984; Ma, 1994; Tang *et al.,* 1995) and the Gangdese porphyry copper belt in southern Tibet (Qu *et al.,* 2001). Preliminary studies have

revealed that the Yulong belt Cu deposits formed in a syn-collisional transpressional environment during the collision. The ore-bearing porphyries of these deposits exhibit features of the shoshonite series (Zhang *et al.,* 1988a, 1988b) and were controlled by a large-scale strike-slip fault system (Hou *et al.,* 2003c). The Gangdese belt Cu deposits formed in a post-collisional extensional environment (Hou *et al.,* 2003a, 2004a). Its ore-bearing porphyries have an adakite magma affinity (Gao *et al.,* 2003; Hou *et al.,* 2003b) and were controlled by a normal fault system intersecting the collision belt (Hou *et al.,* 2004b). Nevertheless, a tectonic model for the formation of porphyry copper deposits in collisional orogenic environments has not yet been constructed.

The key to the construction of such a model must involve understanding: i) the temporal and spatial distribution, and environment of formation of the regional porphyry mineralisation event, ii) mechanisms for the formation of ore-bearing and barren porphyries, and iii) the lithospheric structures in which the porphyry Cu-Mo-Au system originated. Long-term mineral exploration and recent extensive studies have accumulated voluminous information about general framework, spatial-temporal distribution, and features of the porphyry Cu-Mo-Au mineralisation in eastern Tibet, the eastern Indo-Asian collision zone (Rui *et al.,* 1984; Ma, 1994; Bi *et al.,* 1997; Xu *et al.,* 1997; Lo *et al.,* 1998; Hou *et al.,* 2004b). Systematic studies of the >1000 km long alkali-rich porphyry belt in eastern Tibet over many years have greatly increased our understanding of their genetic process and geodynamic setting (Zhang and Xie, 1997; Chung *et al.,* 1998; Deng Wanming *et al.,* 1998a, 1998b; Zhang *et al.,* 2000; J. H. Wang *et al.,* 2001; Wang Jian *et al.,* 2003). Intensive tectonic studies on the Sanjiang Tethys and the eastern collisional zone provide a relatively distinct tectonic framework for the formation of the porphyry Cu-Mo-Au belt (Wang and Buechfiel, 1997; Li *et al.,* 1998; Zhong, 1998). A large amount of geophysical data about this tectonic belt (Lin *et al.,* 1993; Liu *et al.,* 2000; Jiang *et al.,*

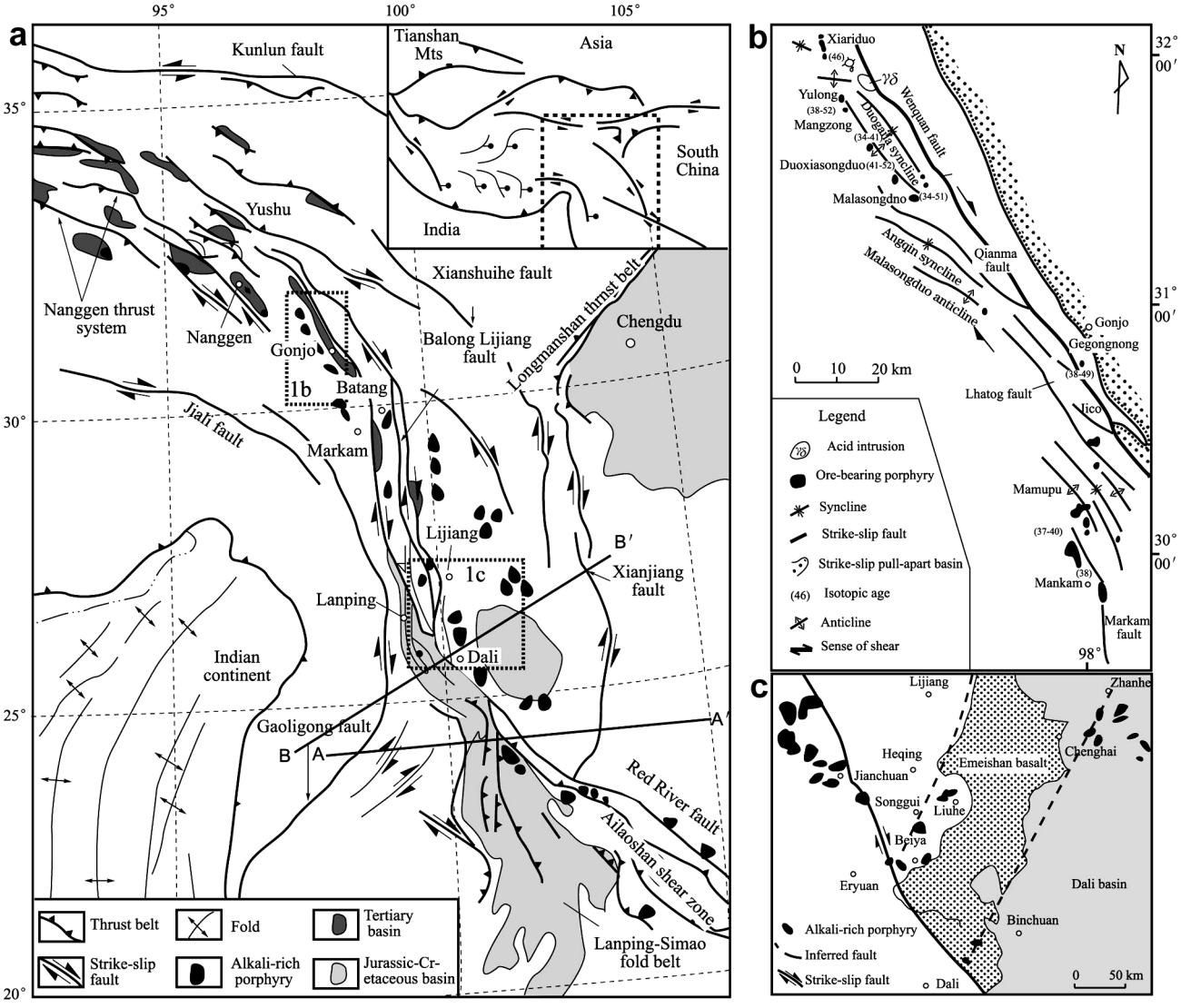

Figure 1: ***Distribution of Cenozoic structure and porphyries in east Tibet from the eastern Indo-Asian collision zone.***

- **a.** The tectonic framework of the eastern Indo-Asian collision zone, east Tibet (modified from Deng *et al.,* 1998a; J-H Wang *et al.,* 2001; Hou *et al.,* 2003e);
- **b.** Structural features and porphyry distribution in the Yulong porphyry copper belt, east Tibet (after Liu *et al.,* 1993 and Hou *et al.,* 2003e);
- **c.** The distribution of porphyry intrusions in the Dali area.

2000; Zhong *et al.,* 2001; Wang Chunyong *et al.,* 2002) provide abundant information for understanding the deep geodynamic processes of the magma genesis, and make it possible for us to discuss and construct a tectonic model for intracontinental porphyry copper deposits.

On the basis of our recent research work, together with data from previous studies, this paper summarises the characteristics of the temporal-spatial distribution of the porphyry copper-molybdenum-gold metallogenic belts, determines the magma affinity and types of ore-bearing and barren porphyries, and discusses the deep processes of their magmatic origin. An attempt is also made to construct a tectonic model for porphyry copper-molybdenum-gold deposits in the eastern Indo-Asian collision zone.

Regional Geological Setting

The study area is located on the eastern margin of the Tibetan Plateau that was formed by the Indo-Asian collision, i.e., the eastern Indo-Asian collision zone. Tectonically, the area is a tectonic transition belt that accommodated the stress-strains produced by that collision. The area underwent a complex tectonic evolution from the Palaeo-Tethys Orogeny in the Palaeozoic-Mesozoic to Himalayan large-scale intracontinental deformation during the Cenozoic (Fig. 1). The Palaeozoic Orogeny was mainly marked by subduction of the Jinshajiang oceanic basin since the late Permian (JS) and development of the Jomda-Weixi arc on the Qiangtang terrane (Mo *et al.,* 1993). Cenozoic deformation was chiefly manifested by Eocene-Oligocene (40-24 Ma) transpressional deformation, early-middle Miocene (24-17 Ma) transtensional deformation, and E-W extension since the Neogene (J-H Wang *et al.,* 2001), forming a number of strike-slip fault systems with various strike directions. Of these fault systems, the western includes the Jiali and Gaoligong strike-slip faults, developed around the eastern Himalayan tectonic syntaxis, while the central consists of the Batang-Lijiang fault in the northern segment and the Ailaoshan-Red River fault on the southern segment. The former of the central system is characterised by N-S trending and right-lateral strike-slip movement, and the latter by NW trending and left-lateral strike-slip movement. Both fault systems constitute a significant boundary between the Yangtze Craton (continental block) on the eastern side, and the Qiangtang terrane on the western side. The eastern system consists of the Longmenshan thrust belt and the Xianshuihe and Xiaojiang strike-slip faults (Fig. 1). Both Cenozoic potassic igneous rocks and a series of early-middle Cenozoic pull-apart basins, such as the Gonju, Jianchuan and Dali basins (Fig. 1), developed

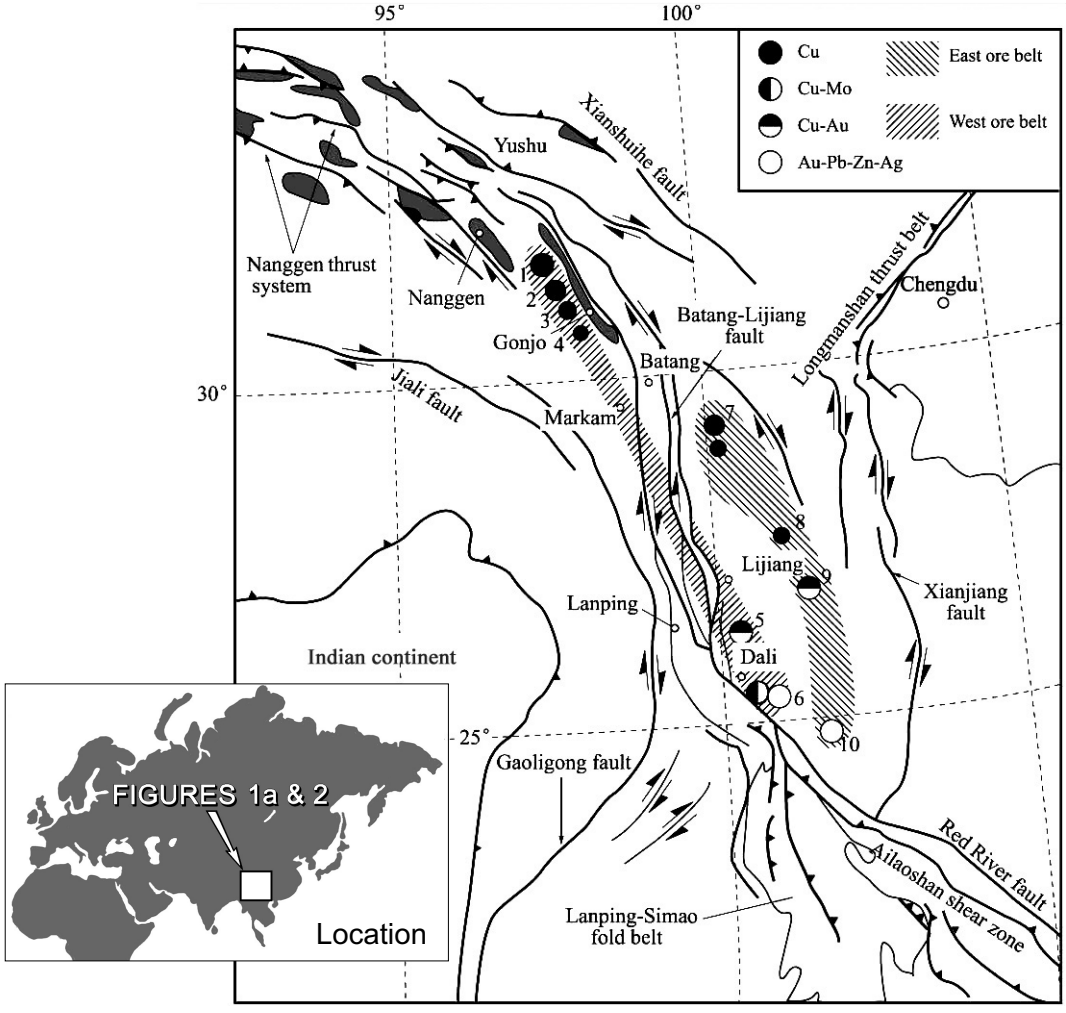

Figure 2: ***A simplified geological map showing the distribution of various porphyry-type deposits in the eastern Indo-Asian collision zone.*** **1.** Yulong Cu deposit; **2.** Malasongduo Cu deposit; **3.** Duoxiasongduo Cu deposit; **4.** Mangzong Cu deposit; **5.** Beiya Au-Cu deposit; **6.** Machangqing Cu-Mo and Au deposit; **7.** Pulang Cu deposits; **8.** Xiaolongtan Cu deposit; **9.** Xifanping Cu-Au deposit; **10.** Yao'an Au-Pb-Zn-Ag deposit.

along a narrow belt following the Nanqian thrust, the Jinshajiang fault system, and the Red River shear zone, forming the huge, >1000 km long, Jinshajiang-Honghe alkali-rich igneous rock belt (Zhang *et al.,* 1998a, 1998b). In this huge magmatic belt, two ore-bearing potassic porphyry belts exist: one (west) is the Jomda-Heqing-Dali alkali-rich potassic porphyry belt, which is distributed along the junction boundary between the Yangtze Craton and Qiangtang terrane and the other (east) is the Zhongdian-Yanyuan-Yao'an alkali-rich potassic porphyry belt, which occurs on the western margin of the Yangtze Craton. Available dating data indicate that the igneous rocks in the western belt yielded ages ranging between 48 and 27 Ma (Lo *et al.,* 1998; Zhang *et al.,* 1998a) and one in the eastern belt has an age range varying from 48 Ma to 31 Ma (Luo *et al.,* 1998).

Porphyry Copper-Molybdenum-Gold Mineralisation

Fig. 2 shows the spatial distribution of major porphyry deposits in the eastern Indo-Asian collision zone. The porphyry deposits may be divided into two metallogenic belts, separated by the Jinshajiang suture (JS). The west belt extends for more than 500 km, from the Jomda in eastern Tibet, southward to the Xiangyun in west Yunnan, including the Yulong porphyry Cu sub-belt in the northern segment, the Beiya porphyry Au-Cu Orefield in the south-central segment and the Machangqing Cu-Mo-Au deposit in the southern segment (Fig. 2). The east belt stretches for more than 300 km from the Zhongdian southward to Yao'an in west Yunnan. Its northern segment is the Pulang (Zhongdian) porphyry Cu mineralisation sub-belt that was found recently, while the central segment is the Xifanping porphyry Cu-Au deposit and the southern segment is the Yao'an porphyry Au-Ag-Pb-Zn deposit (Fig. 2). Generally, the western belt is found in the junction zone of the Yangtze Craton and Qiangtang terrane, controlled by large-scale strike-slip faulting systems. The eastern belt occurs on the western margin the Yangtze Craton, with its northern segment controlled by strike-slip faults and the southern segment constrained by faults inherited from those in the Panxi rift phase. These belts appear to extend southward into Myanmar and mainland SE Asia (Khin Zaw *et al.,* 1999). Both porphyry metallogenic belts have the following similarities:

Similarity in Mineralising Age

The ages of porphyry deposits may be either determined by using accurate molybdenite Re-Os dating or indirectly estimated applying crystallisation age of ore-bearing porphyries. Generally, the formation of porphyry deposits occurred 1-3 Ma before the latest-phase of the intrusion of ore-bearing porphyry bodies (Hou *et al.,* 2003c). In the west belt, the Yulong porphyry Cu sub-belt has molybdenite Re-Os ages of 35.6-35.8 Ma (Du *et al.,* 1994). The age of the Machangqing porphyry Cu-Mo deposit has not yet been directly determined; although, according to the Rb-Sr isochron ages of ore-bearing porphyries, this deposit is estimated to have a mineralisation age of ~ 36.0 Ma (Luo *et al.,* 1998). The mineralisation types of the Beiya porphyry deposit are rather complex. It is estimated, according to the K-Ar age (48 Ma) of the Beiya quartz-syenite porphyry, that the main mineralisation age should be 45±2 Ma. In the east belt, the Xifanping copper-bearing monzonite porphyry has an amphibole $^{40}Ar/^{39}Ar$ plateau age of 47.52 Ma and an isochron age of 46.8 Ma (Luo *et al.,* 1998); hence the mineralising age is estimated at 44±2 Ma. The K-Ar age for the Yao'an syenite porphyry varies from 31 to 50 Ma; on this basis the age of the deposit is estimated to be between 34 Ma and 47 Ma. Though the above data are somewhat speculative, there is a considerable consistency between the mineralising ages of the two-metallogenic belts.

Similarity in Ore-Bearing Porphyry

The similarity is manifested as follows: i) the ore-bearing porphyry associations of the east and west belts are both monzogranite porphyry and monzonite porphyry with a small amount of quartz-syenite porphyry, and spatially, monzogranite porphyry in the north grades southward to monzonite porphyry along both belts; ii) ore-bearing porphyry bodies mostly occur as small stocks and are generally composite rock bodies, resulting from two or more magmatic intrusions; and iii) in a composite intrusion mineralisation is mostly closely related to the more felsic porphyries intruded in the middle and late stages.

Similarity in Wall-Rock Alteration

Wall-rock alteration is mostly centred on an intrusion and developed as rings. Mineralised intrusions normally have a silicified core, which successively passes outward into the K-silicate zone, then to sericite-quartz and finally to a propylitic alteration zone. In the exocontact, marble, hornfels and skarn zones are mostly developed.

Similarity in Mineralisation Features

The similarity is displayed in the following respects: i) their mineralisation features are consistent; ii) Although they occur in an environment which is different from that for porphyry deposits in the circum-Pacific belts, similar mineralisation assemblages appear in the eastern and western belts, i.e. the Cu, Cu-Mo, and Au-Pb-Zn assemblages in the west ore belt and the Cu, Cu-Au, and Au-Pb-Ag assemblages in the east ore belt; and iii) mineralisation types are similar; for example, in most cases veinlet-disseminated mineralisation occurs inside porphyry intrusions, sulphide-rich tabular orebodies in contact zones, and bed-like, lenticular, and veined orebodies in country rocks.

Ore-Bearing & Barren Porphyries

There are over 10 Cenozoic alkali-rich porphyry swarms in the eastern Indo-Asian collision zone, including as many as 1000 separate porphyry bodies. Major element, trace elements and Sr-Nd-Pb isotopic systematics for representative samples from several porphyry bodies have been analysed by many authors (Tables 1 & 2; Ma, 1994; Deng *et al.,* 1998, 1999; Chung *et al.,* 1999; Zhang *et al.,* 1997, 1998a, 1998b, 2000; Wang *et al.,* 2003). To correctly distinguish between ore-bearing and barren porphyries and

to establish corresponding geochemical criteria, we have made a preliminary attempt using our previously published geochemical data on alkali-rich porphyries along the eastern Indo-Asian collision zone.

Fig. 3a compares potassic magmatic rocks developed in different areas of the Tibetan Plateau since the Indo-Asian collision at 60 Ma. Three important facts have been observed: i) most alkali-rich porphyries in eastern Tibet are shoshonitic, although some of them are potassic calc-alkaline, which are characterised by higher SiO_2 contents as compared with the post-collisional potassic-ultrapotassic volcanic rocks in the interior of the Plateau (Turner *et al.,* 1993; Miller *et al.,* 1999); ii) ore-bearing porphyries in eastern Tibet are very similar to those of the Gangdese porphyry belt in southern Tibet, but notably different from those in island arcs, which suggests that the ore-bearing porphyries in the collisional orogenic environment are characterised by high potassium contents; and iii) on the basis of their SiO_2 content, alkali-rich porphyries in eastern Tibet may broadly fall into two groups: a) barren, alkali-rich porphyries with SiO_2 of <63 wt %, predominantly syenite porphyries; and b) mineralised, alkali-rich porphyries with SiO_2 contents of >63 wt %, mainly consisting of granite-, monzogranite-, and monzonite-porphyry, with a small amount of syenite porphyry. In group b), granite porphyry is associated with copper-molybdenum, monzogranite porphyry with copper, monzonite porphyry with copper-gold, and syenite porphyry with gold (-lead-zinc) mineralisation.

Y and Yb are two trace elements that do not participate in mantle inhomogeneity (e.g., mantle metasomatism) and also display incompatible behaviours, remaining stable during alteration (Gill, 1981; Tatsumi, 1986). Unlike both Y and Yb, the high field strength elements (HFSE) (e.g., Nb), show high incompatibility in their geochemical behaviours during magmatic processes, and also remain stable during fluid metasomatism. Therefore, the Nb/Y ratio is free from the influence of fluid metasomatism and may sensitively reflect the enrichment process in a source related to a magmatic melt. In contrast, large ion incompatible elements (LILE) (e.g., Ba) are very active and may be considered key elements indicating fluid metamorphism and enrichment in trace elements. Accordingly, we divide alkali-rich porphyries in the eastern Tibet into these three categories:

Low-Y and low-Ba porphyries

Represented by Cu-bearing porphyries in the Yulong belt, the dominant rocks of this category are monzogranite- and syenogranite-porphyry, generally with <20 ppm Y and <1000 ppm Ba, while Nb/Y varies from 0.35 to 1.25. These Cu-bearing porphyries form a horizontal trend parallel to the Nb/Y axis on Fig. 3a, suggesting that magmatic processes controlled the geochemical variations among different porphyry intrusions or among different porphyry phases.

High-Y and high-Ba porphyries

These are usually barren syenite-porphyries which are widely developed throughout the alkali-rich porphyry belt

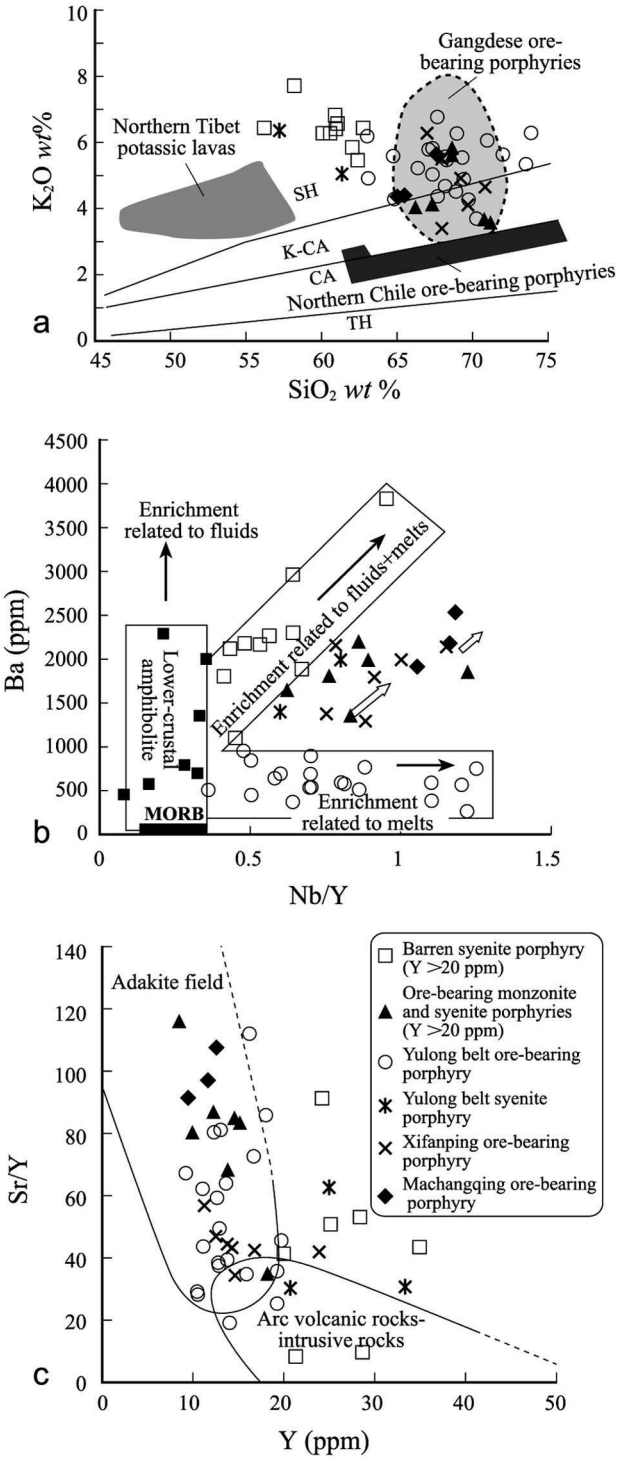

Figure 3: ***Discrimination diagrams for alkali-rich porphyries in east Tibet, the eastern Indo-Asian collision zone.***

- **a.** SiO_2-K_2O diagram of alkali-rich porphyries showing that they are characterised by higher SiO_2 (>63 wt %) and higher potassium, similar to those at Gangdese but different from the potassic lavas of the Plateau.
- **b.** Y-Sr/Y diagram of alkali-rich porphyries illustrating their adakitic affinity (Defant and Drummond, 1990).
- **c.** Ba-Nb/Y diagram of alkali-rich porphyries illustrating that ore-bearing and barren porphyries have different variation trends.

Table 1: ***Major and trace element geochemical data of the representative porphyries from the eastern Indo-Asian collision zone.***

	Low-Y and low-Ba porphyries																
	1	**2**	**3**	**4**	**5**	**6**	**7**	**8**	**9**	**10**	**11**	**12**	**13**	**14**	**15**	**16**	**17**
SiO_2	64.8	67.6	68.9	71	63.1	69.42	67.04	68.94	68.21	68.16	69.3	71.9	73.5	66.4	68.31	67.4	67.29
TiO_2	0.52	0.39	0.35	0.31	0.34	9	0.3	0.27	0.27	0.28	0.28	0.23	0.21	0.22	0.33	0.33	0.42
Al_2O_3	16.4	15.2	15	14.2	18	14.12	14.14	14.26	13.04	14.3	14	13.1	13.3	14.8	15.15	15	14.58
Fe_2O_3	1.23	1.37	1.16	0.54	1.87	1.09	0.94	1.59	1.01	1.02	1.49	1.43	0.66	1.46	1.5	1.22	1.68
FeO	1.76	1.67	1.44	1.5	1.03	1.51	1.1	1.23	2.71	0.43	0.74	1.36	1.38	1	0.82	1.33	1.68
MnO	0.06	0.06	0.07	0.05	0.05	0.15	0.06	0.08	0.12	0.06	0.07	0.12	0.13	0.09	0.1	0.11	0.07
MgO	2.47	1.42	0.79	1.23	1.45	0.83	1.22	1.01	0.99	0.96	1.27	0.63	0.59	1.38	0.99	1.19	1.47
CaO	2.94	2.34	2.83	1.27	2.76	1.86	1.48	1.3	1.67	2.29	0.76	0.65	0.62	0.7	0.99	1.81	2.82
Na_2O	3.77	3.67	3.32	2.87	4.39	3.67	3.27	3.12	2.01	2.82	2.84	2.44	2.95	3.11	3.8	3.31	3.72
K_2O	4.27	4.33	4.52	6.04	4.89	4.85	5.79	6.25	5.57	4.76	5.52	5.6	5.32	5.23	5.45	5.8	5.01
P_2O_5	0.03	0.07	0.11	0.05	0.4	0.1	0.11	0.1	0.11	0.13	0.12	0.13	0.14	0.19	0.12	0.14	0.23
H_2O^+	0.6	0.67	0.54	0.53	1.21	0.5	0.76	1.04	1.32	1.27	1.08	0.78	0.73		0.7	0.97	0.71
Total	98.9	98.9	99	99.5	99.5	98.38	96.21	99.19	97.03	96.48	97.5	98.4	99.6	94.6	98.26	98.6	99.68
La	82.2	67	63	51.9	97.4	45.3	82.11	48.85	32.5	72.76	77.3	60.3	86.3	60.5	57.45	68.7	62.01
Ce	162	123	119	96.4	175	87.09	158.7	86.59	55.5	136.9	143	112	149	108	99.14	122	120.1
Nd	65.9	45.8	45.9	34.4	72.4	33.51	55.28	29.7	20	47.03	50.5	38.2	43.4	43.3	33.05	43.1	45.68
Sm	10.4	7.08	7.36	5.25	10.7	5.56	8.26	4.77	3.6	6.97	7.53	5.51	5.35	6.21	5.32	6.58	7.24
Eu	1.9	1.49	1.52	1.06	2.28	0.97	0.94	0.88	0.78	1.32	1.46	0.88	0.66	1.36	0.95	1.36	1.53
Gd	7.44	5.19	5.45	3.81	6.36	4.41	6.2	3.76	4.2	4.87	5.15	3.98	3.83	3.74	4.21	4.81	5.33
Tb	0.54	0.49	0.4	0.16	0.85	0.39	0.65	0.45	0.78	0.34	0.57	0.31	0.31	0.51	0.43	0.53	0.5
Dy	3.9	2.82	2.99	2.11	3.85	2.98	3.89	2.54	1.9	2.74	2.83	2.27	2.3	2.42	2.5	2.73	2.93
Ho	0.69	0.51	0.59	0.39	0.68	0.58	0.77	0.54	0.62	0.5	0.52	0.4	0.41	0.44	0.43	0.49	0.56
Er	1.89	1.37	1.46	1.07	1.87	1.61	2.07	1.42	0.74	1.45	1.43	1.2	1.27	0.32	1.21	1.37	1.44
Tm	0.29	0.22	0.22	0.14	0.24	0.26	0.35	0.26	0.24	0.24	0.19	0.18	0.19	0.18	0.2	0.25	0.25
Yb	1.52	1.18	1.31	0.94	1.5	1.62	1.92	1.5	1.1	1.3	1.31	1.16	1.17	1.26	1.11	1.2	1.24
Lu	0.28	0.29	0.3	0.19	0.23	0.3	0.36	0.36	0.54	0.26	0.24	0.28	0.2	0.2	0.19	0.32	0.21
Y	16.8	12.4	13.7	9.33	19.7	15.94	19.31	13.88	12.8	12.73	12.9	11.1	10.6	14.2	10.56	12.7	13.15
Sc	8.02	5.12	5.51	4.2		4.84	5	3.53	3.84	3.16	3.65	2.91	1.97		4.12	3.94	5.09
Rb	237	217	225	246	224	229	268	236	240	257	315	203	287	178	269	287	227
Sr	1220	995	878	631	899	559	491	550	480	493	638	486	298	276	306	735	1068
Ba	440	939	636	362	760	571	754	580	740	498	682	379	255	562	678	583	835
Nb	9	6	8	6	72	13	17	15	16	11	9	12	13	17	6	10	7
Ta					0.95									1.37			
Zr	159	113	124	115	288	114	148	101	138	109	101	104	119	242	146	114	94
Hf	19	8	8	9	7	6	15	8	6	4	4	6	5	6	6	6	9
Th	27	29	27	28	20	38	37	36	28	47	48	48	54	32	34	45	38
U																	
Cr																	
Ni																	

1-17: Low-Yand low-Ba porphyries, predominantly monzogranite porphyries; samples **1-5** from the Yulong bodies; **6-9** from the Malasongdo bodies; **10-14** from the Duoxiasongduo bodies; **15-16** from the Zhanaga bodies; **17** from the Mangzong bodies.

18-27: Low-Y and medium-Ba porphyries. - Sample **18-19** from the Xifanping district (quartz monozite porphyries); **20-21** from the Machangqing district (**20:** granitic porphyry; **21:** quartz-syenitic porphyry); **22-25:** from the Beiya district (quartz-syenitic porphyries); **26:** syenitic porphyry in the Jianchuan; **27:** syenitic porphyry in the Liuhe

Table 1: ***Continued***

	Low-Y and medium-Ba porphyries										High-Y and high-Ba syenitic porphyries											
	18	**19**	**20**	**21**	**22**	**23**	**24**	**25**	**26**	**27**	**28**	**29**	**30**	**31**	**32**	**33**	**34**	**35**	**36**	**37**	**38**	**39**
SiO_2	65.47	65.04	69.72	66.94	68.63	62.73	66.24	70.74	67.32	68.64	60.95	60.56	62	60.07	57.36	71.23	73.9	67.7	45.54	46.38	51.55	39.08
TiO_2	0.42	0.39	0.32	0.29	0.19	0.71	0.34	0.3	0.39	0.27	0.77	0.65	0.62	0.47	0.59	0.27	0.22	0.22	0.72	0.54	0.97	3.13
Al_2O_3	15.3	15.57	15.18	14.94	16.16	14.04	15.5	14.8	15.71	14.94	14.24	14.26	14.53	14.18	14.31	13.54	13	15.6	13.93	13.81	17.89	16.15
Fe_2O_3	1.89	1.88	1.12	1.22	1.37	2.72	1.68	1.36	2.11	1.15	2.1	1.92	1.84	2.34	2.38	1.18	0.63	1.71	4.3	4.06	4.36	3.61
FeO	1.69	1.44	1.18	1.18	0.35	4.81	1.6	0.98	0.88	0.47	2.7	2.59	2.32	1.77	2.82	1.03	1.06	1.13	7.13	7.77	4.33	10.58
MnO	0.17	0.07	0.05	0.07	0.03	1.09	0.07	0.04	0.06	0.04	0.09	0.1	0.09	0.1	0.11	0.47	0.07	0.07	0.24	0.32	0.29	0.11
MgO	1.52	1.59	0.8	1	0.18	0.23	1.67	0.54	1.08	0.36	2.51	2.65	2.46	2.3	2.77	1.32	0.07	1.77	11.26	10.32	3.96	12.9
CaO	2.19	2.29	1.6	2.9	1.14	0.48	2.8	1.93	2.43	1.94	4.76	4.77	4.01	3.69	4.41	1.98	0.97	0.65	10.6	11.02	6.54	1.83
Na_2O	5.16	4.85	4.03	3.08	4.95	0.26	4.56	4.58	4.89	4.96	3.33	3.91	4.19	3.87	3.34	4.22	2.36	2.68	2.24	2.06	4.36	0.95
K_2O	4.37	4.36	4.1	6.3	5.81	6.45	4.02	3.69	4.13	5.6	6.39	6.34	5.84	6.28	6.56	3.57	6.29	6.75	1.56	1.23	3.64	8.21
P_2O_5	0.28	0.21	0.13	0.11	0.07	0.24	0.19	0.14	0.18	0.09	0.42	0.39	0.39	0.3	0.39	0.18	0.1	0.22	0.12	0.14	0.27	1.06
H_2O^+	1.22	1.61	0.9	0.76		1.23	0.59	0.04			1.27						0.46	1.09				
Total	99.68	99.3	99.13	99.31	99.69	99.52	99.46	99.52	99.96	99.27	99.55	99.51	99.46	99.75	99.5	99.49	99.13	99.6	99.98	99.48	99.47	99.69
La	70.66	81.76	47.85	53.3	16.28	30.68	27.28	16.16	42.06	45.69	33.44	35.81	32.83	51.75	49.43	53.03	79.75	61	11.91	11.5	26.5	73
Ce	126.9	127.5	84.88	73.7	26.79	52.88	50.37	35.49	78.59	83.12	61.94	66.88	61.97	94.91	97.37	94.3	152.1	117	16.74	12.02	69.48	182.8
Nd	46.8	51.31	29.79	33.4	11.35	19.84	22.37	14.42	29.95	30.72	26.52	26.95	25.47	36.97	41.36	34.71	64.93	47.4	9.68	8.46	48.58	82.72
Sm	8.18	7.2	4.9	5.2	2.37	3.66	4.31	2.75	5.9	5.47	5.1	5.41	4.82	7.34	8.67	5.72	10.32	7.36	2.58	2.03	13.79	16.28
Eu	1.75	1.63	1.03	1.04	0.93	1.24	1.22	0.86	1.61	1.79	1.5	1.75	1.71	2.21	2.63	1.89	2.32	1.84	0.92	0.83	2.79	3.2
Gd	4.84	4.48	3.48	3.44	2.49	3.14	3.55	2.23	5.26	4.84	4.4	4.59	5.2	6.36	8.93	5.11	6.76	5.26	2.56	2.52	12.26	15.08
Tb	0.58	0.59	0.46	0.44	0.29	0.46	0.46	0.28	0.62	0.52	0.61	0.71	0.71	0.85	1.12	0.64	0.93	0.71	0.4	0.45	2.21	2.04
Dy	2.73	2.43	2.07	1.94	1.57	2.44	2.33	1.36	2.97	2.65	3.19	3.69	3.55	4.8	5.9	2.92	4.41	3.53	2.33	3.09	12.7	9.19
Ho	0.51	0.46	0.41	0.47	0.32	0.48	0.45	0.25	0.5	0.53	0.63	0.64	0.75	0.87	1.08	0.48	0.79	0.67	0.49	0.68	2.53	1.5
Er	1.21	1.12	1	1.02	0.76	1.23	1.18	0.65	1.32	1.32	1.666	1.86	2.05	1.54	2.79	1.26	2.26	1.91	1.33	1.56	7.68	3.58
Tm	0.18	0.17	0.15	0.26	0.13	0.18	0.18	0.1	0.16	0.17	0.26	0.23	0.27	0.34	0.4	0.15	0.3	0.26	0.17	0.18	1.11	0.41
Yb	1.11	1.08	0.94	0.85	0.83	1.11	1.18	0.65	1.18	0.98	1.64	1.56	1.88	2.31	2.59	0.94	1.93	1.72	1.21	1.38	6.14	1.82
Lu	0.16	0.17	0.14	0.29		0.16	0.19	0.11			0.25		0.25			0.19	0.29	0.27	0.19	0.21	0.97	0.27
Y	12.61	11.36	14.2	12.5	10	13.21	14.52	8.48	15.18	13.82	19.96	18.23	20.35	25.15	28.45	12.16	23.85	20.8	12.58	15.78	63.09	32.35
Sc			4	3.3		2.13	5.23	1.81			10.6											
Rb	134	137	158	218	241.4	325.4	105.7	89.71	134.8	253.6	211.4	220.5	211.3	270.8	231.8	131.2	124.6	293	49.43	34.64	70.14	302
Sr	708	1332	616	590	805.6	70.51	1231	983.8	1266	943.8	831.4	641.6	646.7	1285	1517	1059	1 002	628	346.1	311.1	124	224.7
Ba	1787	2148	1368	2130	1848	592.6	1637	1353	1980	1796	2303	2969	2069	1884	2267	2194	524	893	568	444.6	2294	2006
Nb			10.7	14.4	12.21	24.63	8.93	7	13.54	10.57	12.8	11.71	15	16.78	15.99	10.5	17	15	2.01	1.28	13.47	12.06
Ta		0.56			0.71	1.41	0.63	0.5	1.04	0.56	0.7	0.48	0.74	1.08	1.08	0.67	1.33	1.22	0.11	0.08	0.71	7.92
Zr	306	349	40.8	70.2	310.9	222.2	148	131.1	398.8	200.4	207.1	229.1	233.9	515.8	415.2	253.2	265	267	79.95	72.13	234.6	456.4
Hf	5.3	6.5			4.19	6.48	4.35	4.12	5.05	5.11	5.5	5.86	5.42	5.68	4.76	5.72	7	7	1.28	1.14	5.6	9.77
Th	28.17	28.41	26.3	28.9	12.31	10.71	10.83	6.13	16.49	14.04	2.87	9.29	10.21	28.62	19.99	22.86	34	33	3.11	1.71	2.01	18.41
U	2.6	3.4	13.3	9.3	2.15	3.61	3.55	5.6	4.29	2.37	2.87	2.47	3.52	8.93	6.37	4.87			0.41	0.35	1.47	3.02
Cr	111	150	39.8	16.8	11.43	99.13	273.7	222.3	14.54	120.4	235	72.62	68.03	85.54	80.08	42.39			148.2	156.1	49.24	220.2
Ni	36	30	21.6	15.6	0.81	39.65	132.6	114.2	5.9	38.76	133.1	37.02	31.9	37.35	36.22	22.3			87.19	70.1	17.14	139.7

28-35: High-Y and high-Ba syentic porphyries. - Sample **28-30** from the Liuhe; **31-32** from the Jianchuan; **33** from the Zhanhe; **34-35** from the Mangzong.

36-39: Amphibolite xenoliths. - Sample **36-38** from the Liuhe, **39** from the Dali. Samples **36-37** are no-plagioclase amphibolites, **38** and **39** are plagioclase-bearing amphibolites plagioclase-bearing amphibolites.

in the eastern Indo-Asian collision zone. Their Y content is commonly >20 ppm, while Ba is usually > 1000 ppm, varying from 1000 to 4000 ppm. Although the Nb/Y ratios of these porphyries also vary from 0.35 to 1.25, these ratios form a Nb/Y-Ba positive correlation trend (Fig. 3b), implying the combined control of both subducted-slab fluid metasomatism and magmatic processes.

Low-Y and medium-Ba porphyries

The Y content of this group is generally similar to that of the low-Y and low-Ba porphyries, varying from 10 to 20 ppm, while Ba is usually >1000 ppm. The representative intrusives are granite-, monzonite- and quartz-syenite-porphyries. Of these, granite porphyry occurs in the Machangqing Cu-Mo ore district; monzonite porphyry is developed in the Xifanping Cu-Au ore district; and quartz-syenite porphyry is mainly developed in the Beiya and Yao'an Au or Au-Ag ore districts. Compared with the low-Y and low-Ba porphyries, their mineralisation potential is slightly poorer. In Fig. 3b this group usually lies between the variation trends for low-Y, low-Ba porphyries and those with high-Y, and high-Ba. However, a positive Nb/Y-Ba correlation trend is also observed, suggesting that their sources experienced similar fluid metasomatism, but that the degree of fluid metasomatism and trace element enrichment is higher than those of low-Y, low-Ba porphyries.

In Fig. 3c the magmatic affinities of ore-bearing porphyries and barren porphyries are further distinguished. The great majority of ore-bearing porphyries lie in the adakite field (Defant and Drummond, 1990), whereas barren syenite porphyry is located outside the adakite field. A typical example is the Yulong porphyry Cu sub-belt, where mineralised monzogranite (syenogranite) porphyry and a small amount of quartz-syenite porphyry with lower Y and higher Sr/Y lie in the adakite field, while the barren syenite porphyry with higher Y content plots outside the adakite field. In addition, such features as higher SiO_2 (>63 wt %) and higher Al_2O_3 (>15 wt % with SiO_2 = 65 wt %), strong fractionation between LREE and HREE, and no negative Eu anomaly for the ore-bearing porphyries also suggest that they have an adakitic affinity (Defant and Drummond, 1993). However, compared with typical adakite, the ore-bearing porphyries in the study area are high in potassium and enriched in LILE. We call these ore-bearing porphyries "adakite-like" rocks.

Similar "adakite-like" rocks have been reported in the Andean arc orogenic belt, the largest porphyry Cu belt in the world (Oyarzun *et al.,* 2001). Two metallogenic belts have been recognised in northern Chile (Sillitoe, 1982). One is the arc-related calc-alkaline porphyry Au-Cu belt, dominated by epithermal Au-Cu deposits, and the other is the adakitic porphyry Cu belt, in which a considerable number of large and super-large porphyry Cu deposits occur (Sillitoe, 1982; Oyarzun *et al.,* 2001). The reserves of copper metal in adakitic porphyry Cu belts are ten times larger than those in normal calc-alkaline belts (Oyarzun *et al.,* 2001). In the Gangdese porphyry Cu belt of southern Tibet, the ore-bearing porphyries are also adakitic, but show high-K characteristics (Hou *et al.,* 2003b). The ore-bearing porphyries in eastern Tibet are generally similar to the Gangdese porphyries, except for relatively high abundances of LILE and Y. The geochemical similarities of porphyries hosting Cu deposits in arc and collisional zones indicate that "adakite-like" rocks have a significant ore potential (Hou *et al.,* 2003b).

Genesis of Alkali-Rich Porphyries

Many models have been proposed for the genesis of alkali-rich porphyries in eastern Tibet, including partial melting of an enriched mantle (Zhang *et al.,* 2000), or the melting of the crust-mantle transition zone (Deng Wanming *et al.,* 1998a, 1998b; Zhong *et al.,* 2001) related to eastward subduction of the continental slab along the Red River fault (J-H Wang, *et al.,* 2001), or the partial melting of an "island arc-type" mantle induced by large-scale strike-slip movement (Hou *et al.,* 2003c; Wang Jian *et al.,* 2003). However, any model must explain the following four important facts: i) the temporal-spatial association between alkali-rich porphyry intrusions and lamprophyres and between ore-bearing adakitic porphyry and barren syenite porphyry; ii) geochemical characteristics such as LILE enrichment, HFSE depletion, and Nd-Sr homogenisation of alkali-rich porphyries and their associated rocks; iii) the control of lithosphere-scale strike-slip fault systems on temporal-spatial localisation of alkali-rich porphyries; and iv) the geodynamic setting characterised by subduction of the Yangtze block at about 50 Ma and upwelling of asthenospheric material beneath eastern Tibet (Liu *et al.,* 2000; Zhong *et al.,* 2001). The porphyry genesis is further constrained by the xenoliths hosted by the porphyry intrusions, and the trace element geochemistry and Sr-Nd-Pb isotopic systematics of alkali-rich porphyries.

Constraint from Deep-Seated Xenoliths

In the alkali-rich porphyries and their associated lamprophyres, two different kinds of xenoliths have been found, i.e., upper-mantle xenoliths and lower-crustal xenoliths. The major upper-mantle xenoliths are phlogopite harzburgite, found in potassic lamprophyres at Muli, Yanyuan, and Dali (Lu and Zheng, 1998), which suggests that the lamprophyres are derived from the hydrous upper mantle. The lower-crustal xenoliths dominantly comprise amphibolite, garnet amphibolite, and eclogite which are recognised in syenite- and monzonite-porphyry at Jianchuan, Liuhe, and Dali (Cai, 1992; Deng *et al.,* 1998a, 1998b; Wang Jian *et al.,* 2003). These xenoliths demonstrate that the lower crust in eastern Tibet underwent shortening and thickening (>40 km) during the Indo-Asia collision. The primary rocks were probably basaltic in composition (Deng *et al.,* 1998a), which had been metamorphosed during the collision to garnet amphibolite and/or eclogite, which are usually considered an ideal source for adakitic melts (Defant and Drummond, 1990; Drummond *et al.,* 1996). Of course, the fact that they are hosted in alkali-rich porphyries might also imply that monzonite- and syenite-porphyries may have originated at the top of the upper mantle and were brought up during magmatic segregation, uplift and emplacement.

Based on the mineral assemblages in the xenoliths, there are two types of lower crust amphibolites, i.e., those containing, and those without, plagioclase, with the former being relatively enriched in LILE and HFSE and the latter being relatively depleted in these elements (Deng *et al.,* 1998a). On the Ba-Nb/Y diagram (Fig. 3b), the Nb/Y ratios of both amphibolites are equivalent, but the former is characterised by higher Ba, while the latter is closer to MORB. These features suggest that the lower crust in eastern Tibet is chemically heterogenous, possibly reflecting a difference in the degree of fluid metasomatism. Plagioclase-bearing amphibolite shows a higher degree of fluid metasomatism and enrichment, whereas plagioclase-free amphibolite indicates a slightly lower degree of metasomatism and enrichment. Assuming the fluids participating in the metasomatism originated from the ancient subducted slab (Hou *et al.,* 2003c; Wang Jian *et al.,* 2003), then plagioclase-bearing amphibolites should lie vertically below plagioclase-free amphibolites. This suggestion is obviously contrary to the metamorphic facies transformation for lower-crustal rock at >400 km depth. The simultaneous occurrence of two types of xenoliths in the same porphyry swarm possibly implies that the variation in chemical composition of the lower crust is mainly lateral, i.e., the slab fluid metasomatism led to the geochemical inhomogeneity at the base of the lower crust, which is also manifested in the Sr, Nd and Pb isotopic compositions (Fig. 5a).

Constraint from Trace Elements

Although divergent views exist as to the genesis of alkali-rich porphyries, it has been generally accepted that alkali-rich porphyries have the following geochemical characteristics: i) alkali-rich porphyries are relatively enriched in LILE, such as K, Rb, Ba, and Sr, and relatively depleted in HFSE, such as Nb, Ta, P, and Ti, showing geochemical characteristics similar to those of the island arc-type magma source (Fig. 4a); ii) the REE pattern is LREE-enriched, and LREE and HREE exhibit strong fractionation but no pronounced negative Eu anomalies (Fig. 4b); and iii) the less evolved alkali-rich porphyries have a slightly intermediate composition but are relatively enriched in transition elements (Cr, Ni, Co) that are usually enriched in basic magmas. These characteristics have an important constraint on their genesis.

It is more reasonable to suggest that subducted slab fluid metasomatism and enrichment has occurred in the source rather than to consider that the source of the alkali-rich porphyries has had "island arc-type" geochemical characteristics. This is because: i) the fluids produced by the dehydration of a subducted slab will carry large quantities of mobile elements (e.g., LILE), metasomatising the overlying mantle wedge and making it highly enriched in LILE (Tastumi, 1996); ii) partial melting under hydrous conditions tends to cause the Nb-, Ta-, Ti-, and P-bearing mineral phases such as rutile to remain stable in the source (Tastumi, 1996) so that their melts are relatively enriched in LILE but strongly depleted in HFSE; and iii) the dehydrated subducted slab may be either an oceanic slab rich in seawater (ODP Leg 110 Scientific Party, 1987) or a continental slab rich in formation water (Oliver, 1992; Johnston, 1999). In eastern Tibet, both slab-types appeared in different periods of time. The Jinshajiang oceanic slab was subducted westward during the Permian, forming the Jomda-Weixi volcanic arc (Mo *et al.,* 1993) and the Yangtze continental slab was subducted westward in the Cenozoic and induced the upwelling of asthenospheric material (Liu Futian *et al.,* 2000; Zhong *et al.,* 2001). The question of which type of slab caused the fluid metasomatism remains to be further constrained by isotope data.

Alkali-rich porphyries usually exhibit no pronounced negative Eu anomalies, but are relatively enriched in Sr. Conversely, this suggests that the porphyry magma is not a residual melt evolved after the segregation and crystallisation of plagioclase from mantle-derived primitive basaltic magma, i.e., the porphyry itself should represent an independent magma with an intermediate composition. However, this also indicates that the magma source contains either minimal amounts of plagioclase or no plagioclase at all. In other words, the possible source for alkali-rich porphyries is either amphibolite and/or garnet amphibolite or hydrous upper mantle.

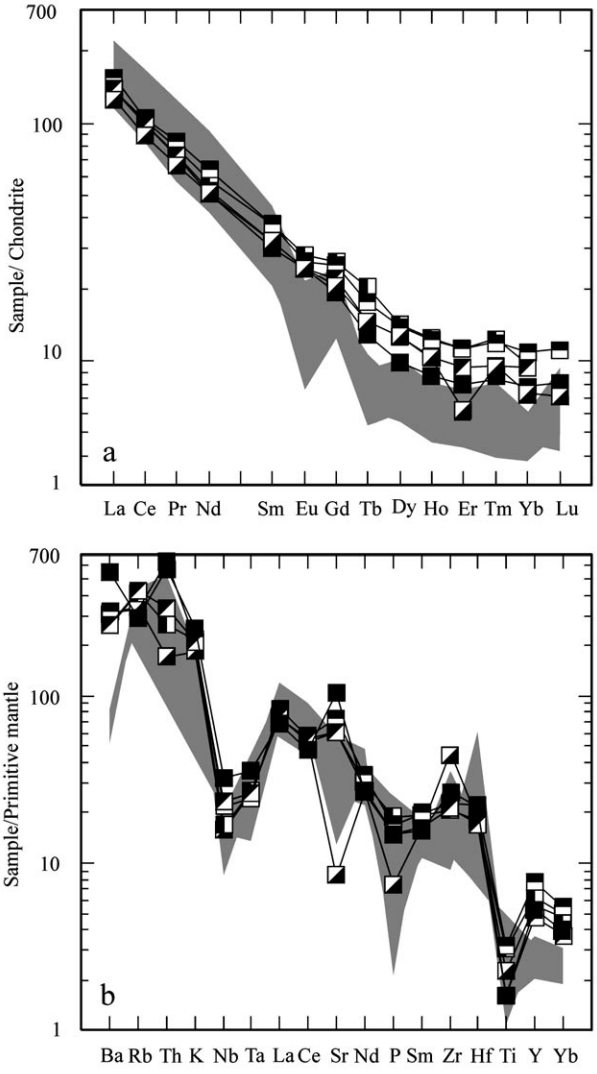

Figure 4: a). ***REE patterns,*** *and* **b).** ***trace element abundance patterns,*** for alkali-rich porphyries in east Tibet, the eastern Indo-Asian collision zone. Shadow fields are ore-bearing, others are barren alkali-rich porphyries.

The Y content of porphyries is an important criterion for determining whether a garnet mineral phase existed. The reason why adakite with low Y and an intermediate-acid composition is generally considered to have been derived from partial melting of eclogite caused by the metamorphism of basaltic rocks, is that the Y-rich garnet mineral phase is preserved in a stable form in the source during the partial melting process (Defant and Drummond, 1990). The "adakite-like" rocks represented by the Yulong ore-bearing porphyries has <20 ppm Y, suggesting that their source should be amphibolite or garnet amphibolite. The lower-crustal xenoliths are typical representatives of such source rock. Although the LILE-enriched and HFSE-depleted characteristics of these porphyries reveal important information on metasomatism of the magma source by subducted slab fluids, the geochemical modification of the magma is little affected by the slab fluids, possibly due to the control by the enrichment process related to melts (Fig. 3b). High-Y syenite porphyry is high in Ba, Rb, and K and low in Ti and Nb. These features suggest that the

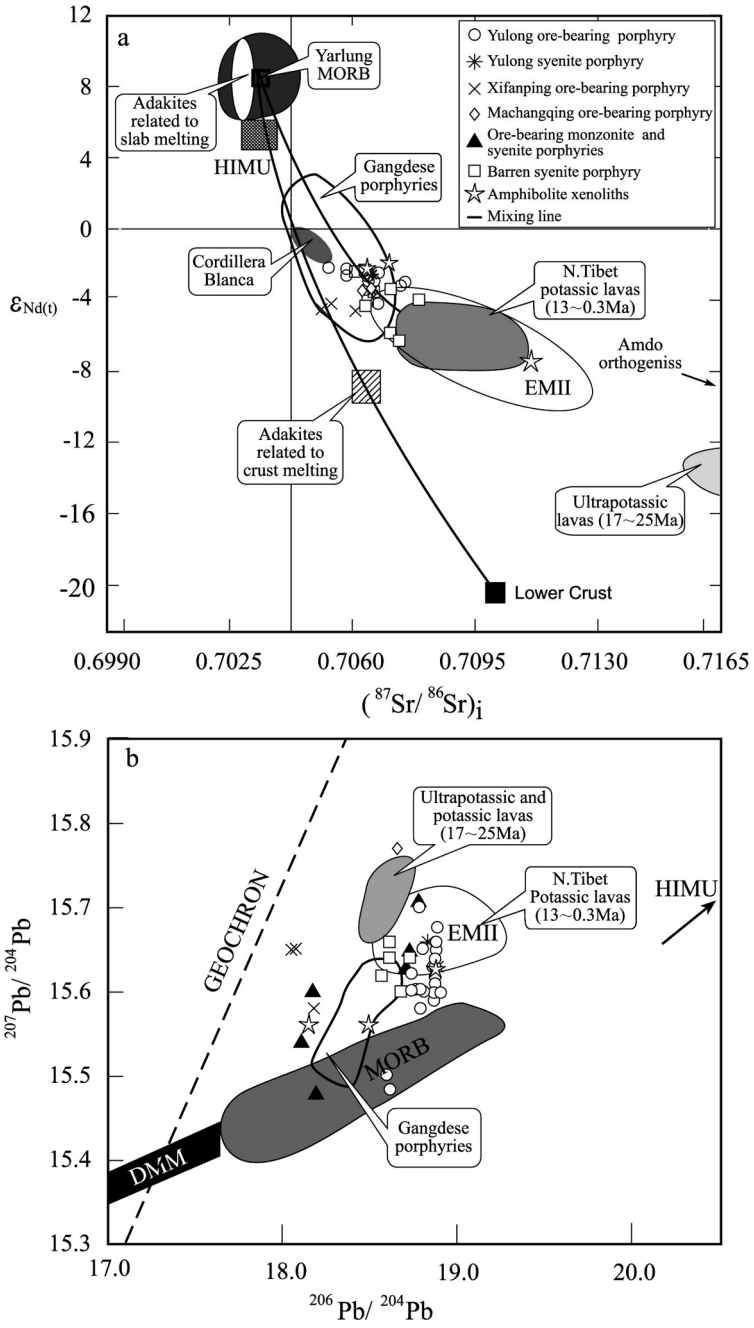

Figure 5: ***Sr-Nb-Pb isotopic systematics of alkali-rich porphyries in the eastern Indo-Asian collision zone.***

a. Nd and Sr isotopic compositions of alkali-rich porphyries and lower-crustal xenoliths. *Data sources:* adakite related to slab melting from Defant and Drummond (1993), Kay *et al.,* (1993), and Stern *et al.,* (1996); adakite related to crust melting from Xu *et al.,* (2001). Gangdese ore-bearing porphyries from Hou *et al.,* (2004a); potassic and ultra-potassic lavas in north Tibet from Turner *et al.,* (1993); Cordillera Blanca adakite from Petford and Atherton (1996).

b. Pb isotopic composition of alkali-rich porphyries and lower-crustal xenoliths. The east and west porphyry metallogenic belts show two different variation trends. *Data source:* potassic and ultra-potassic lavas in north Tibet from Turner *et al.,* (1996); Gangdese ore-bearing porphyries from Hou *et al.,* (2004b).

garnet mineral phase possibly did not exist in its source, which should therefore be hydrous upper-mantle. The mantle-derived xenoliths of "phlogopite harzburgite" in lamprophyres are possibly its typical representatives of such a source. It is especially noteworthy that the positive Ba-Nb/Y correlation trend formed by these high-Y porphyries (Fig. 3b) implies that the geochemical changes to syenite-porphyry are possibly controlled by two kinds of enrichment processes: one is enrichment associated with melts (the Nb/Y ratio increase), while the other is the process of fluid metasomatism. The former process might be related to discontinuous upward infiltration of melts from the asthenosphere (McKenzie, 1989) (see the next section); whereas the latter process is related to the dehydration of the ancient subducted slab (Wang Jian *et al.,* 2003). However, it is not yet clear whether the source was metasomatised again by fluids derived from the subducted Yangtze continental slab.

Constraint from Sr-Nd-Pb Isotopes

The interpretation arising from studies of deep-seated xenoliths and trace element geochemistry are strongly supported by the Sr-Nd-Pb isotope systematics of the porphyries (Table 2). Fig. 5 shows that the initial Nd, Sr, and Pb isotopic compositions of both alkali-rich porphyries and potassic lamprophyres are different, not only from the isotope-depleted asthenospheric mantle (MORB) but also from the normal crust. Based on these isotopic signatures, Deng Wanming *et al.,* (1998a, 1998b) proposed that the type II enriched mantle (EM II), formed by mixing of subducted oceanic crust and upper mantle, is probably an ideal source melt for the production of alkali-rich porphyries. Wang Jian, *et al.,* (2003) suggested that a mantle wedge, subjected to metasomatism by fluids derived from the ancient Jinshajiang subduction slab, became an "island arc-type" mantle to produce the alkali-rich porphyry magma. In comparison, we consider that the crust-mantle transition zone, metasomatised by subducted slab fluids and mixed with asthenospheric material, is a likely source for alkali-rich porphyries in eastern Tibet.

This crust-mantle transition zone shows lateral and vertical inhomogeneity in trace element and isotopic geochemistry. Vertically, in the lower part of the transition zone, it comprises hydrous mantle peridotite with EM II characteristics due to strong metasomatism by subducted slab fluids. The partial melting of the lower part of the transition zone, triggered by the input of asthenospheric material, might have produced high-Y syenite magma, which fall in between EM II and MORB on the $(^{87}Sr/^{86}Sr)_i$ - Nd diagram (Fig. 5a). In the upper part of the transition zone, the basaltic lower-crust is metamorphosed to amphibolite and garnet-amphibolite as a result of crustal shortening and thickening during the Himalayan collisional orogeny. Moreover, the lower-crust in the transition zone also experienced slab-derived fluid metasomatism and the input of small volumes of asthenospheric melts. The lower-crustal samples brought up by magmas display appreciable variations in Sr, Nd, and Pb isotopic compositions, which never the less plot between EM II and MORB and coincide with the isotopic compositions of low-Y porphyries (Fig. 5). Laterally, the crust-mantle transition zone also shows geochemical inhomogeneity, manifested most obviously by the Pb isotopic composition (Fig. 5b). The $^{260}Pb/^{204}Pb$ ratios of ore-bearing and barren alkali-rich porphyries vary between 18.078 and 18.205 in the east belt and between 18.576 and 18.908 in the west belt. In Fig. 5b they form two separate, sub-vertical arrays, with one end approaching MORB and the other tending towards EM II. These variation features imply that the magmatic sources for the east belt had undergone much larger-scale contamination by asthenospheric material, compared with those from the west belt.

Deng Wanming *et al.,* (1998b) inferred that the source of alkali-rich porphyries in eastern Tibet formed at ~220-250 Ma, based on the lead isotope study of alkali-rich porphyries in western Yunnan. Wang Zeng *et al.,* (1995) also reached a similar conclusion for the Yulong copper-bearing porphyries, based on the estimation of the Nd model ages of 200-240 Ma. This suggests that large-scale regional fluid metasomatism in the source is possibly related to the westward subduction of the Late Palaeozoic Jinshajiang oceanic slab, which gave rise to an embryonic source for alkali-rich porphyry magmas (Fig. 6a). On the other hand, the input of asthenospheric material into the source, and its consequent contamination, are possibly related to the upwelling of the asthenosphere, triggered by the subduction of the Indian and Yangtze continents toward each other (Fig. 6b). This has been also supported by deep geophysical exploration data.

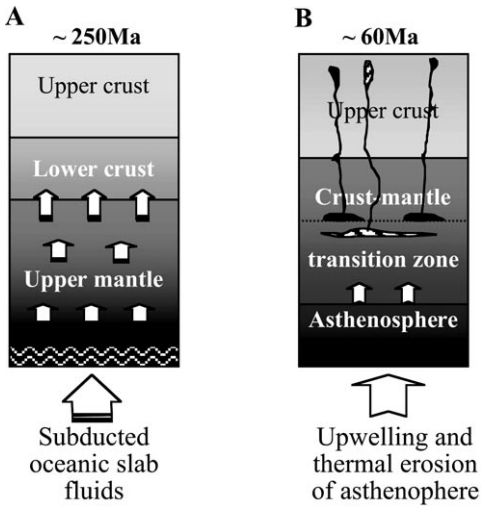

Figure 6: ***Diagrams illustrating the evolutionary processes of the alkali-rich porphyry source in the eastern Indo-Asian collision zone.***

A. Metasomatism of the lithosphere by the underlying Jinshajiang subducted oceanic slab fluids since ~250 Ma.

B. A complex crust-mantle transition zone was formed by upwelling and thermal erosion of the lithosphere induced by the subduction of the Yangtze continental block and input of a small stream of melts. This zone is a possible source region of alkali-rich porphyries.

Table 2: *Sr-Nd-Pb isotopic systematics of the representative porphyries from the eastern Indo-Asian collision zone.*

Location	Rocks	$^{206}Pb/^{204}Pb$	$^{207}Pb/^{204}Pb$	$^{208}Pb/^{204}Pb$	$^{143}Nd/^{144}Nd$	ε_{Ndt}	$^{87}Sr/^{86}Sr$	δSr
Porphyries in the West Ore Belt								
Yulong[b]	Monzogranite porphyry	18.757	15.642	38.903	0.512427±19	-4.2	0.706765±8	32.2
		18.779	15.642	38.924	0.512525±11	-2.2	0.706576±11	29.5
		18.733	15.626	38.890				
		18.890	15.682	39.119				
		18.608	15.488	38.528				
		18.805	15.648	38.866				
Malasongduo[b]	Monzogranite porphyry				0.512473±9	-3.2	0.706832±10	33.1
		18.826	15.608	38.872				
		18.888	15.643	38.955				
		18.864	15.615	38.869				
Duoxiasongduo[b]	Monzogranite porphyry				0.512492±14	-2.8	0.706576±8	29.5
		18.852	15.634	38.915	0.512532±11	-2.1	0.705453±20	13.5
		18.871	15.622	38.920				
		18.867	15.586	38.799				
		18.788	15.583	38.801				
		18.869	15.627	38.911				
		18.852	15.634	38.915				
Zhanaga[b]	Monzogranite porphyry	18.867	15.661	38.963	0.512509±9	-2.5	0.705817±21	18.7
	Syenitic-granite porphyry	18.870	15.648	38.955	0.512485±8	-3.0	0.705997±9	21.2
Mangzong[b]	Monzogranite porphyry	18.883	15.629	38.921	0.512522±9	-2.3	0.706329±14	26.0
Mamupu[b]	Syenitic porphyry	18.825	15.659	38.958	0.512496±10	-2.5	0.706191±6	24.0
					0.512464±8	-3.4	0.706212±8	24.3
Beiya[a]	Quartz-syenitic porphyry	18.652±1	15.586±3	38.646±5	0.512380±15	-4.6	0.707455±21	0.70719
		18.791±2	15.706±4	38.992±1	0.512409±16	-4.0	0.707614±18	0.70737
		18.702±2	15.634±6	38.781±13	0.512440±8	-3.4	0.707361±30	0.70655
		18.714±1	15.649±4	38.824±14	0.512395±17	-3.3	0.708070±36	0.70752
		18.605±2	15.637±6	38.899±1	0.512296±26	-6.3	0.707968±25	0.70756
		18.583±2	15.618±3	38.787±8	0.512319±21	-5.8	0.707799±39	0.70729
Machangqing [a]	Syenitic porphyry	18.670	15.773	39.754	0.512460±8	-3.5	0.706499±5	29.8
					0.512464±9	-3.4	0.706871±12	35.1

Table 2: *Continued from previous page.*

Location	Rocks	$^{206}Pb/^{204}Pb$	$^{207}Pb/^{204}Pb$	$^{208}Pb/^{204}Pb$	$^{143}Nd/^{144}Nd$	ε_{Ndt}	$^{87}Sr/^{86}Sr$	δSr
Porphyries in the East Ore Belt								
Yao'an [d]	Syenitic granite porphyry	18.094	15.537	38.682				
		18.205	15.478	38.834				
		18.177	15.609	38.951				
		18.177	15.609	38.951				
Xifanping [c]	Quartz monozite porphyry	18.082	15.645	38.401	0.512409±24	-4.1	0.705703±25	
		18.078	15.644	38.467	0.512384±24	-4.5	0.705467±26	
Zhanhe [a]	Monozite porphyry	18.174±21	15.579±19	38.342±8	0.512376±13	-4.6	0.706488±20	26.4
Barren alkali-rich rocks								
Nanqen[b]	Trachyte	18.908±17	15.608±14	38.996±35	0.512597±11	-0.84	0.705739±	17.6
Zongguo[b]	Trachyte	18.861±9	15.659±11	38.965±17	0.512552±16	-1.7	0.705187±9	9.8
Midu[b]	Trachyte	18.730±6	15.599±5	38.776±14	0.512630±10	-0.2	0.706759±6	32.1
Xiaoguancun[b]	Trachyte	18.564±6	15.552±13	38.408±16	0.512403±25	-0.2	0.706759±6	32.1
Lijiang[b]	Pyroxene syenite	18.678	15.601	38.664	0.512517±8	-2.4	0.706519±11	30.1
Binchuan[b]	Pyroxene syenite	18.576	15.514	38.664	0.512463±16	-3.4	0.706244±8	26.2
					0.512544±39	-1.8	0.706360±14	27.8
Dali[b]	Alkali syenite				0.512536±13	-2.0	0.705677±7	18.1
					0.512487±50	-2.9	0.705488±9	15.0
Lower-crust xenoliths								
Liuhe [a]	Amphibolite	18.846 ±1	15.631±3	39.191±7	0.512240±18	-7.4	0.711559±25	68.8
		18.136±1	15.557±1	37.839±3	0.512540±13	-1.9	0.707356±25	37.8
Dayingjie [a]	Amphibolite	18.480±5	15.562±8	38.431±9	0.512511±6	-2.4	0.706759±25	29.4

Data source: a. Deng *et al.(*1998); **b**. Zhang *et al*. (1997) and Zhang *et al*. (2000); **c**. Xu *et al. (*1997); **d**. Luo *et al.* (1998)

Deep Crust-Mantle Structure and Magmatic Processes

Using deep geophysical data, Zhong *et al.,* (2001) have considered that the spatial distribution of Cenozoic magmatic rocks in eastern Tibet was constrained by mantle upwelling, whereas alkali-rich, potassic magma originated from partial melting of the crust-mantle transition zone. Here we will further discuss the relationship of formation of alkali-rich porphyry magmas with subduction of the Yangtze block and upwelling of the asthenosphere, mainly on the basis of the tomographic data.

Fig. 7 presents two composite interpretative cross-sections deduced from seismic tomographic data, combined with regional tectonics. Though the two sections have different azimuths, they transect similar tectonic units and reveal very consistent information of the deep lithospheric structure. The nearly E-W section at 23.5°N shows that the Indian and the Yangtze continental slabs are subducted toward each other (Zhong *et al.,* 2001). The Indian continental slab, which appears west of the Jiali-Gaoligong strike-slip fault (94°- 97° E), is subducted at a gentle angle beneath the Tethys-Himalaya; the subducted front reaching 96°- 97° E, then suddenly plunging down and extending sub-vertically to a depth of 180 km (Jiang *et al.,* 2000; Wang Chunyong *et al.,* 2002). The Yangtze continental slab appears east of the Jiali-Gaoligong strike-slip faults (99°-102° E). This slab is subducted westward at a gentle angle along the Red River strike-slip fault, and at around 100°-E the angle of the subducted slab becomes steep and plunges down, reaching a depth of 250 km (Fig. 7a; Liu *et al.,* 2000). At the NE-directed velocity perturbation section, the image of the subducted Yangtze continental slab is still clearly visible, and the slab also steepens suddenly at 100°- 99° E, with its front reaching a depth of almost 300 km (Fig. 7b; Zhong *et al.,* 2001).

The subduction of the Yangtze and Indian continental slabs toward each other, and successive oblique collision between the Indian and Asian continents since 60 Ma, may have induced the upwelling of asthenospheric material in eastern Tibet. Seismic tomographic imaging has verified that in the area (97°- 99° E) between the fronts of the two subducted slabs there is an occurrence of a notably low-velocity upwelling of the asthenosphere derived from 450 km depth and its continuation took place at a depth of 200-250 km. From 200 km upward, the upwelling led to a significant thinning of the overlying continental lithosphere to 70-80 km and was underplated laterally eastward, causing a decrease in the seismic velocities of the upper mantle and lower crust (Liu *et al.,* 2000). Underneath the modern Tengchong volcanic area, the underplated basaltic magmas derived from asthenosphere thermally corroded away most of the overlying lithospheric mantle (Zhong *et al.,* 2001).

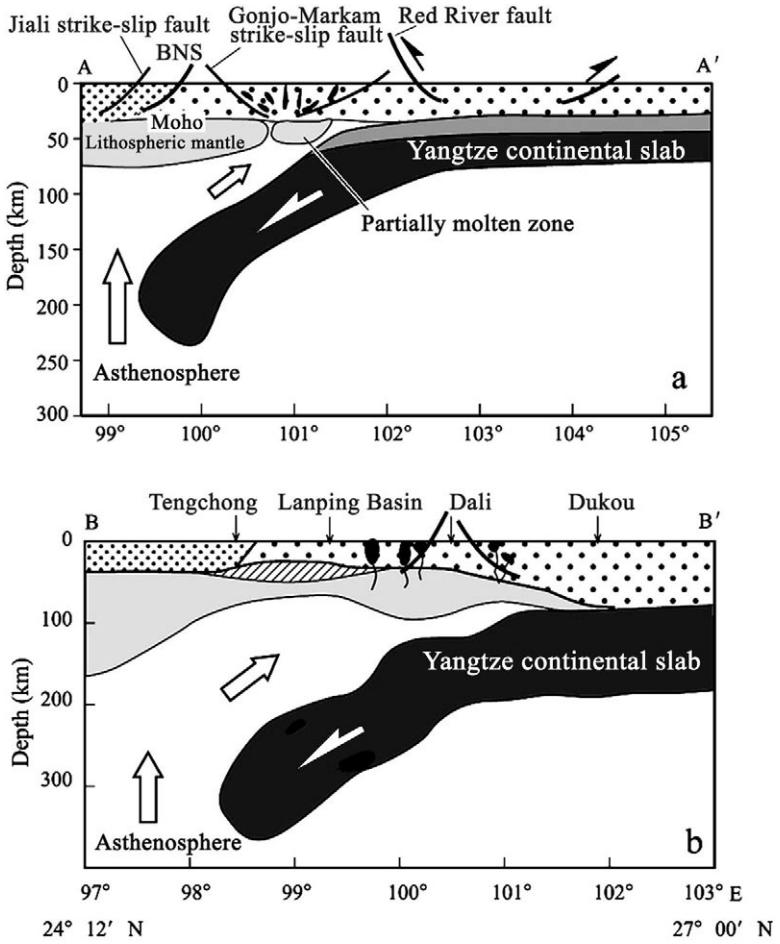

Figure 7: ***Lithospheric structure beneath the eastern margin of the Plateau*** inferred from the tomographic image data and surface geological structure. For the locations of sections A-A′ and B-B′, see Fig l. For the tomographic image data of section A-A′, see Liu *et al.,* (2000). For the data of the velocity perturbation section (section B-B′), see Zhong *et al.,* (2001).

It seems that upwelling and underplating of hot asthenosphere provided the necessary heat energy for partial melting of the source to form the alkali-rich magmas. Furthermore, the infiltration and input of asthenospheric melts into the overlying lithosphere supplied a "brand" of MORB components at the crust-mantle transition zone and in its magmatic products.

A Possible Tectonic Model for Porphyry Cu-Mo-Au Deposits

Two different tectonic models have been proposed for the formation of the Cenozoic igneous rocks and associated porphyry Cu-Mo-Au deposits in the Indo-Asian collision zone, based on the study of tectono-magmatic processes of the alkali-rich porphyry belt (Chung *et al.,* 1998; Zhong *et al.,* 2001; Wang J-H. *et al.,* 2001). Chung's model emphasises that the formation of the alkali-rich magmas in eastern Tibet were attributed to the convection and thinning of lithospheric mantle, triggered by the post-collisional crustal extension and partial melting of subcontinental enriched mantle in eastern Tibet (Chung *et al.,* 1998). Based on the peak age of alkali-rich magmas, Chung *et al.,* (1998) inferred that the uplift of the eastern margin of the Plateau reached a maximum height before 40 Ma. The transpressional tectonic model proposed by Zhong *et al.,* (2001) suggested that the alkali-rich magmas originated from small-scale upwellings of the asthenosphere and partial melting of the crust-mantle transition zone in an intra-continental transpressional environment. They consider that, at least before 40 Ma, the eastern margin of the Plateau was in a long-term transpressional regime, which was replaced by regional extension at ~20 Ma (J-H Wang *et al.,* 2001). Our new observations and interpretation on the regional structure and magmatism, along with the above-mentioned geophysical data, support the second model.

The key to the construction of a tectonic model for porphyry Cu-Mo-Au deposits in the Indo-Asian collision zone is to understand the origin of the ore-bearing adakite-like rocks. Several genetic models for the formation of adakite have been proposed, including, i) partial melting of subducted oceanic crust (Peacock and Rusher, 1994; Sajona *et al.,* 2000), ii) partial melting of the mafic lower-crust (Petford and Atherton, 1996; Xu *et al.,* 2002), and iii) assimilation and fractional crystallisation (AFC) of basaltic magmas (Castillo *et al.,* 1994). The ore-bearing porphyries in eastern Tibet reveal information about metasomatic fluids from the Jinshajiang subducted oceanic slab, although deep geophysical data has not detected such a subducted slab in the depth range (48-60 km) within which the porphyry magma originated. Even though the westerly-subducted Jinshajiang oceanic slab may act as a possible source for the ore-bearing porphyries in eastern Tibet, this cannot explain the genesis of the ore-bearing porphyries in the east metallogenic belt that occurs in the interior of the Yangtze block. Multiple intrusions of the ore-bearing porphyries in eastern Tibet suggest that their parent magma underwent crystallisation, differentiation and even crustal contamination; however, the small compositional variation and no pronounced Eu anomaly within the ore-bearing porphyries indicate that the AFC process is not the leading mechanism for generation of adakitic porphyries; on the contrary, deep-seated xenolith, trace element, and isotope geochemical evidence all indicate that the ore-bearing porphyries were derived from mafic lower-crust that underwent metasomatism of the components from the subducted slab and input of asthenospheric material at depth. As a result of thickening (to >40 km) caused by the Indo-Asian continent collision after 60 Ma, the mafic lower-crust had probably been transformed into amphibolite and /or garnet-amphibolite and their partial melting may have given rise to adakitic melts.

The heat energy inducing partial melting of the mafic lower-crust was either derived from underplating of the basaltic magma at depth (Petford and Atherton, 1996), or upwelling of the hot asthenosphere generated by delamination of the lithosphere (Xu *et al.,* 2002). Upward injection of asthenospheric melts and the thermal erosion of the upwelling asthenosphere, as indicated by the tomographic imaging in eastern Tibet, might have resulted in melting of the lower crust. However, upwelling of the asthenosphere was not induced by the large-scale delamination of the lithosphere, but by the subduction of the Indian continent and Yangtze block toward each other. The top of the upwelling asthenosphere does not have an extensive "mushroom" shape, but takes the form of a zonal upright "tile sheet" (Zhong *et al.,* 2001). This spatial shape of the upwelling asthenosphere fundamentally constrains the huge belt-shaped distribution of alkali-rich porphyries and their associated volcanic lavas. Melts from the top of the asthenosphere might have occurred as small streams of magma injecting into the lower crust and mixing with the lower-crustal material. Such a process resulted in relative enrichment in Mg and the transition elements such as Cr, Ni, and Co of the ore-bearing porphyries.

The adakitic magma produced by partial melting of the lower crust that had been metasomatised by slab fluids and injected by asthenospheric material is a possible carrier of some metals (Cu, Au, Mo etc.) and sulphur for porphyry Cu-Mo-Au deposits (Hou *et al.,* 2003b). This is because: i) the adakitic magma produced by the hydrous source region exhibits the features of a "wet magma" and has strong potential for segregation and production of magmatic ore fluids; ii) the adakitic magma is relatively enriched in sulphur (Oyarzun *et al.,* 2001), with higher oxygen fugacity (fO_2) buffered by the nickel/nickel oxide and hematite/ magnetite buffers (Imai *et al.,* 1993), which would have caused an increase in the SO_2/H_2S ratio in the magmatic system, thus completely removing sulphur from the adakitic melts (Burnham, 1979); and iii) the input of asthenospheric material into the adakitic magma source also causes the melts to obtain large amounts of metals and sulphur effectively from more mafic melts (Hatttori and Keith, 2001).

Based on the integration of the above analyses, we propose a tectonic model for porphyry Cu-Mo-Au deposits in collisional orogenic belts (Fig. 8). Our model emphasises that subduction of a continental slab during a collisional orogeny results in crustal shortening and thickening, and

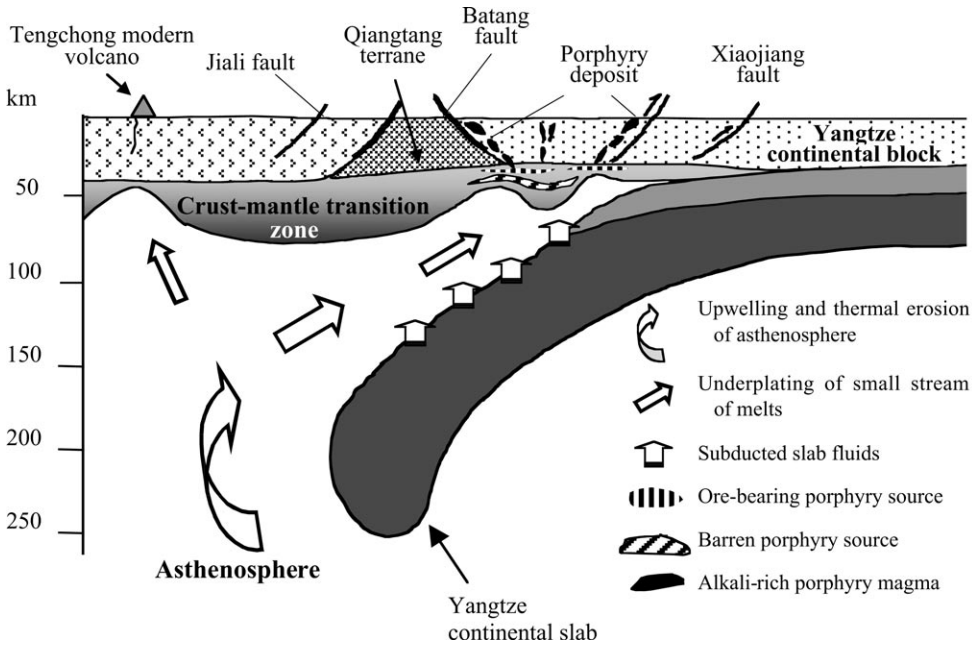

Figure 8: ***A possible tectonic model for porphyry Cu-Mo-Au deposits in the eastern Indo-Asian collision zone.***

triggers upwelling of the asthenosphere. The crust-mantle transition zone that underwent strong metasomatism by ancient oceanic slab fluids was subjected to partial melting under the effects of the tectono-thermal erosion of the asthenosphere and input of a small stream of melts and continental crustal slab fluids. Melting of hydrous phlogopite peridotite in the lower part of the transition zone produced barren syenite-porphyry magmas, whereas melting of hydrous garnet amphibolite in the lower crust gave rise to the ore-bearing adakitic magmas. These porphyry magmas were emplaced at a shallow level along strike-slip faults at their intersections with basement faults, while the ore-bearing magmatic fluids were segregated in a local extensional and stress release regime, which finally evolved into a porphyry magmatic-hydrothermal ore-forming system. Copper-rich fluids might have been segregated from more felsic monzogranite porphyry magmas, forming porphyry copper deposits; whereas gold (and lead-zinc) rich fluids might have been segregated from more intermediate quartz monzonite porphyry magmas, generating porphyry gold deposits.

Acknowledgments

This study was supported by the project "Metallogeny of Collisional Orogeny in Tibet" (No. 2002CB412600) to implement the State Plan for Development of Basic Research.

References

Burnham, C.W., 1979 - Magma and hydrothermal fluids. *in* Barnes, H.L., (Ed.), Geochemistry of Hydrothermal Ore Deposits, 2nd ed.: *Wiley,* New York, pp. 71–136.

Camus, F. and Dilles, J.H., 2001 - A special issue devoted to porphyry copper deposits of northern Chile-Preface: *Economic Geology,* v. 96, pp. 233–238.

Castillo, R.P., Pringle, M.S. and Carlson, R.W., 1994 - East Mariana basin tholeiites: Cretaceous intraplate basalts or rift basalts related to the Ontong Java plume?: *Earth and Planetary Science Letter,* v. 123, pp. 139–154.

Chung Sun-Lin, Lo Ching Hua, Tung-Yi Lee, *et al.,* 1998 - Dischronous uplift of the Tibetan plateau starting from 40 My ago: *Nature,* v. 349, pp. 769–773.

Defant, M.J. and Drummond, M.S. 1990 - Derivation of some modern arc magmas by melting of young subducted lithosphere: *Nature,* v. 347, pp. 662–665.

Defant, M.J., 1993 - Mount St. Helens: potential example of partial melting of subducted lithosphere in a volcanic arc. *Geology,* v. 21, pp. 547–550.

Deng Wanming, Huang Xuan, Zhong Dalai, 1998a - Petrological characteristics and genesis of Cenozoic alkali-rich porphyries in eastern Yunnan. *Scientia Geologica Sinica,* v. 33, pp. 412–425 *(in Chinese with English abstract).*

Deng Wanming, 1998b - Alkali-rich porphyries in the northern segment of the Jinshajiang belt, western Yunnan, and their relations to intraplate deformation: *Science in China (Series D),* v. 28, pp. 111–117 *(in Chinese)*.

Deng Jinfu, Zhao Hailing, Mo Xuanxue, *et al.,* 1996 - Root-Column Structure of the Continent of China - a Key to Continental Geodynamics: *Geological Publishing House,* Beijing *(in Chinese).*

Ding Jianchao, Wang Zeng and Shentu Baoyong, 1990 - Nd-Sr isotope features of major ore-forming intrusions in the Yulong porphyry Cu (Mo) belt, eastern Tibet: *in* CGQXT Editorial Committee, Ministry of Geology and Mineral Resources (Ed.), Contributions to the Geology of the Qinghai-Xizang (Tibet) Plateau, No. 20: *Geological Publishing House,* Beijing, pp. 160–167 *(in Chinese with English abstract).*

Drummond, M.J., Defant, P.K. and Kepezhinskas, 1996 -

Petrogenesis of slab-derived trondhjemite-tonalite-dacite/adakite magmas: *Transactions of the Royal Society of Edinburgh, Earth Sciences,* v. 87, pp. 205–215.

Du Andao, He Hongliao and Yin Wanning, 1994 - The study on the analytical methods of Re-Os age for molybdenites: *Acta Geologica Sinica,* v. 68, pp. 339–346 *(in Chinese with English abstract).*

Gao Yongfeng, Hou Zengqian, Wei Ruihua, 2003 - Petrology and geochemistry of Neogene Gangdese porphyries and their geodynamic significance: *Acta Petrologica Sinica,* v. 19 (3), pp. 418-428 *(in Chinese with English abstract).*

Griffiths, J.R. and Godwin, C.I., 1983 - Metallogeny and tectonics of porphyry copper-molybdenum deposits in British Columbia: *Canadian Journal of Earth Science,* v. 20, pp. 1000-1018.

Hattori, K.H. and Keith, J.D., 2001 - Contribution of mafic melt to porphyry copper mineralization: evidence from Mount Pinatubo, Philippines, and Bingham Canyon, Utah, USA: *Mineralium Deposita,* v. 36, pp. 799–806.

Hou, Z-Q., Qu, X-M., Wang, S-X., *et al.,* 2003a - Re-Os ages of molybdenite in the Gangdese porphyry copper belt, Qinghai-Tibet Plateau: timing of mineralization and application of the dynamic background: *Science in China,* v. 32, pp. 509-618 *(in Chinese).*

Hou, Z-Q., Mo, X-X., Gao, Y-F, Qu, X-M. and Meng, X-J., 2003b - Adakite, a possible host rock for porphyry copper deposits: A case study of porphyry copper belts in Tibetan Plateau and in northern Chile: *Mineral Deposits,* v. 22 (1), pp, 1–12 *(in Chinese with English abstract).*

Hou, Z-Q., Ma, H-W., Khin Zaw and Zhang, Y-Q., 2003c - The Himalayan Yulong porphyry copper belt: product of large-scale strike-slip faulting in eastern Tibet: *Economic Geology,* v. 98, pp. 125–145.

Hou, Z-Q., Meng, X-J., Qu, X-M., *et al.,* 2004a - Gangdese adakitic porphyry copper belt in Tibet*: Acta Petrologica Sinica,* v. 20, pp. 239-248 *(in Chinese with English abstract).*

Hou, Z-Q., Gao, Y-F., Qu, X-M,. Rui, Z-Y. and Mo, X-X., 2004b - The mid-Miocene adakitic rocks generated during the east-west extension in south Tibet: *Earth and Planetary Science Letter,* v. 220, pp. 139-155.

Imai, A., Listanco, E.L. and Fujii, T., 1993 - Petrologic and sulfur isotopic significance of highly oxidized and sulfur-rich magma of Mount Pinatubo, Philippines: *Geology,* v. 21, pp. 699–702.

Jiang Chaosong, Wang Shaojin, Zhou Ruiqi, *et al.,* 2000 - Dynamic study of the Tengchong volcanic active structure: *Seismological Research,* v. 23, pp. 179–187 *(in Chinese with English abstract).*

Johnston, J.D., 1999 - Regional fluid flow and the genesis of Irish Carboniferous base metal deposits: *Mineralium Deposita,* v. 34, pp. 571–598.

Kay, S.M., Ramos V.A. and Marquez M., 1993 - Evidence in Cerro Pampa volcanic rocks for slab-melting prior to ridge-trench collision in Southern South America: *Journal of Geology,* v. 101, pp. 703-714.

Li, X-Z., Liu, W-J., Wang, Y-Z. and Zhu, Q-W., 1999 - The tectonic evolution of the Tethys and mineralisation in the Sanjiang, southwestern China: *Geological Publishing House,* Beijing, 258p. *(in Chinese with English abstract).*

Lin Zhongyang, Hu Hongxiang, Zhang Wenbin, *et al.,* 1993 - Study of the characteristics of the velocity structures of the crust and upper mantle in western Yunnan: *Acta Seismologica Sinica,* v. 15, pp. 427–440 *(in Chinese).*

Liu Futian, Liu Jianhua, He Jiankun and You Q-Y, 2000 - The subducted slab of the Yangtze continental block beneath the Tethyan orogen in western Yunnan: *China Science Bulletin,* v. 45, pp. 466–469.

Lo Yaonan, *et al.,* 1998 - Longmanshan-Jinpingshan intracontinental orogenic belt. *Science and Technology Publishing House,* Chengdu, Sichuan, 171p. *(in Chinese).*

Lu Fengxiang and Zheng Jianping, 1998 - Mantle petrology of China since the 1990s: retrospect and prospect: *in* Ouyang Ziyuan (Ed.), Retrospect and Prospect of Mineralogy, Petrology and Geochemistry at the Turn of the Century. *Atomic Energy Publishing House,* Beijing, pp. 118–122 *(in Chinese).*

Ma, H-W., 1990 - Granitoids and mineralization of the Yulong porphyry copper belt in eastern Tibet. *China University of Geosciences Press,* Beijing, 157p. *(in Chinese with English abstract).*

Miller, C., Schuster, R., Klotzli, U., Frank, W. and Purtscher, F., 1999 - Post-collisional potassic and ultrapotassic magmatism in SW Tibet: geochemical and Sr-Nd-Pb-O isotopic constraints for mantle source characteristics and petrogenesis: *Journal of Petrology,* v. 40, pp. 1399–1424.

Mitchell, A.H.G., 1973 - Metallogenic belts and angle of dip of Benioff zones: *Nature,* v. 245, pp. 49–52.

Mo, X-X., Lu, F-X,. Shen, S-Y., Zhu, Q-W. and Hou, Z-Q., 1993 - The Tethyan volcanism and mineralization in the Sanjiang region: *Geological Publishing House,* Beijing, 250 p. *(in Chinese with English abstract).*

ODP Leg 110 Scientific Party, 1987 - Expulsion of fluids from depth along a subduction zone decollement horizon: *Nature,* v. 326, pp. 785–788.

Oliver, J., 1992 - The spots and stains of plate tectonic: *Earth Science Reviews,* v. 32, pp. 77–106.

Oyarzun, R., Marquez, A., Lillo, J,. Lopez, I. and Rivera, S., 2001 - Giant versus small porphyry copper deposits of Cenozoic age in northern Chile: adakitic versus normal calc-alkaline magmatism: *Mineralium Deposita,* v. 36, pp. 794–798.

Peacock, S.M., Rusher, T. and Thompson, A.B., 1994 - Partial melting of subducting oceanic crust: *Earth and Planetary Science Letter,* 121: pp 224–227.

Petford, N. and Atherton, M., 1996 - Na-rich partial melts from newly underplated basaltic crust: the Cordillera Blanca batholith, Peru: *Journal of Petrology,* v. 37, pp. 1491-1521.

Qu Xiaoming, Hou Zengqi, Gao Yongfeng, *et al.,* 2001 -

Gangdese porphyry copper belt: the second "Yulong porphyry copper belt in Tibet?: *Mineral Deposits,* v. 20 (3), pp. 355–366 *(in Chinese with English abstract).*

Rui, Z-Y., Huang, C-K., Qi, G-M., Xu, J. and Zhang, M-T., 1984 - The porphyry Cu (-Mo) deposits in China: *Geological Publishing House,* Beijing, 350p. *(in Chinese with English abstract).*

Sajona, F.G., Maury, R.C. and Pubellier, M., 2000 - Magmatic source enrichment by slab-derived melts in a young post-collision setting, central Mindanao (Philippines): *Lithos,* v. 54, pp. 173–206.

Sillitoe, R.H., 1972 - A plate tectonic model for the origin of porphyry copper deposits: *Economic Geology,* v. 67, pp. 184-197.

Sillitoe, R.H., Camus, F., (Eds.), 1991 - A special issue devoted to gold deposits in the Chilean Andes: *Economic Geology,* v. 86, pp. 1153–1345.

Stern, C.R. and Kilian, R., 1996 - Role of the subducted slab, mantle wedge and continental crust in the generation of adakites from the Andean Austral Volcanic Zone: *Contributions to Mineral Petrology,* v. 123, pp. 263-281.

Tang, R-L. and Luo, H-S., 1995 - The geology of Yulong porphyry copper (molybdenum) ore belt, Xizang (Tibet): *Geological Publishing House,* Beijing, 320p. *(in Chinese with English abstract).*

Tapponnier, P., Lacassin, R., Leloup, P.H., *et al.,* 1990 - The Ailao Shan/Red River metamorphic belt: Tertiary left-lateral shear between Indochina and South China: *Nature,* v. 343, pp. 431–437.

Tatsumi, Y., 1986 - Chemical characteristics of fluid phase released from a subduction lithosphere and origin of arc magma: evidence from high-pressure experiments and natural rocks: *Journal of Volcanology and Geothermal Research,* v. 29, pp. 293–309.

Turner, S., Hawkesworth, G., Liu, J., Rogers, N., Kelley, S. and Calsteren, P.V., 1993 - Timing of Tibetan uplift constrained by analysis of volcanic rocks: *Nature,* v. 364, pp. 50–54.

Wang Chunyong, Lou Hai, Wu Jianping, Bai Xhiming, Huangfu Gang and Qin Jiazheng, 2002 - Seismological study on the crustal structure of the Tengchong volcano-geothermal area: *Acta Seismologica Sinica,* v. 24 (3), pp. 230–240 *(in Chinese with English abstract).*

Wang, E. and Buechfiel, B.C., 1997 - Interpretation of Cenozoic tectonics in the right-lateral accommodation zone between the Ailao Shan shear zone and the eastern Himalayan syntaxis. *International Geology Review,* v. 39, pp. 191–219.

Wang, J., Li, J-P. and Wang, J-H., 2003 - Shoshonitic magmatism in Dali-Jianchuan area, western Yunnan: a geochemical study of arc magmatism in a post-collisional strike-slip extensional setting: *Acta Petrologica Sinica,* v. 19 (1), pp. 61–71 *(in Chinese with English abstract).*

Wang, J-H., Yin, A., Harrison, T.M., *et al.,* 2001 - A tectonic model for Cenozoic igneous activities in the eastern Indo-Asian collision zone: *Earth and Planetary Science Letter,* v. 88, pp. 123–133.

Wang, Z., Shentu, B-Y., Ding, J-C., Yao, P., and Geng, Q-R., 1995. Granitoid and its mineralization in the eastern Tibet, China: *Southwestern University of Communication Press,* Chengdu*,* 150p. *(in Chinese with English abstract).*

Xu, J.F., Shinjo, R., Defant, M.J., Wang, Q. and Rapp, R.P., 2002 - Origin of Mesozoic adakitic intrusive rocks in the Ningzhen area of east China: partial melting of delaminated lower continental crust?: *Geology,* v. 30, pp. 1111–1114.

Xu Shijing, Shen Weizhou, Wang Rucheng, Lu Jianjun, Lin Yinping, Ni Pei, Luo Yaonan and Li Lizhu, 1997 - Characteristics and origin of the Xifanping porphyry copper deposit, Yanyuan County, Sichuan Province: *Acta Mineralogica Sinica,* v. 17, pp. 56–62 *(in Chinese with English abstract).*

Zhang, Y-Q. and Xie, Y-W., 1997 - Chronology and Nd-Sr isotopes of the Ailaoshan-Jinshajiang alkali-rich intrusions: *Science in China,* v. 27, pp. 289–293 *(in Chinese).*

Zhang, Y-Q., Xie, Y-W. and Li, X-H., 2000 - Isotope features of magmatic rocks of the shoshonitic series in the eastern Qinghai-Tibet Plateau: origin of the rocks and their tectonic significance: *Science in China (Series D),* v. 30, pp. 493–498 *(in Chinese).*

Zhang, Y-Q., Xie, Y-W., Qiu, H-N., Li, X-H. and Zhong, S-L., 1998a - Petrogenesis series and the ore-bearing porphyries of the Yulong copper ore belt in eastern Tibet: *Geochimica,* v. 27, pp. 236–243 *(in Chinese with English abstract).*

Zhang, Y-Q., 1998b - Shoshonitic series: Sr, Nd, and Pb isotopic compositions of ore-bearing porphyry for the Yulong copper ore belt in eastern Tibet: *Scientia Geologica Sinica,* v. 33, pp. 359–366 *(in Chinese with English abstract).*

Zhong Dalai (Ed.), 1998 - Paleotethyan Orogenic Belt in Yunnan-Western Sichuan: *Science Press, Beijing,* 232p. *(in Chinese).*

Zhong, D-L., Ding, L., Liu, F-T., Liu, J-H., Zhang, J-J., Ji, J-Q. and Chen, H., 2001 - The poly-layered architecture of lithosphere in the orogen and its constraint on Cenozoic magmatism: *Science in China,* v. 30, pp. 1-8 *(in Chinese).*